

Article

Thermal Properties of Aliphatic Polypeptoids

Corinna Fetsch ^{1,2} and Robert Luxenhofer ^{1,2,*}

¹ Professur für Makromolekulare Chemie, Department Chemie, Technische Universität Dresden, Zellescher Weg 19, 01062 Dresden, Germany

² Functional Polymer Materials, Chair of Chemical Technology of Materials Synthesis, University Würzburg, Röntgenring 11, 97070 Würzburg, Germany; E-Mail: corinna.fetsch@uni-wuerzburg.de

* Author to whom correspondence should be addressed;

E-Mail: robert.luxenhofer@uni-wuerzburg.de; Tel.: +49-0931-3189930; Fax: +49-0931-3182109.

Received: 19 December 2012; in revised form: 18 January 2013 / Accepted: 21 January 2013 /

Published: 29 January 2013

Abstract: A series of polypeptoid homopolymers bearing short (C_1 – C_5) side chains of degrees of polymerization of 10–100 are studied with respect to thermal stability, glass transition and melting points. Thermogravimetric analysis of polypeptoids suggests stability to >200 °C. The study of the glass transition temperatures by differential scanning calorimetry revealed two dependencies. On the one hand an extension of the side chain by constant degree of polymerization decrease the glass transition temperatures (T_g) and on the other hand a raise of the degree of polymerization by constant side chain length leads to an increase of the T_g to a constant value. Melting points were observed for polypeptoids with a side chain comprising not less than three methyl carbon atoms. X-ray diffraction of polysarcosine and poly(*N*-ethylglycine) corroborates the observed lack of melting points and thus, their amorphous nature. Diffractograms of the other investigated polypeptoids imply that crystalline domains exist in the polymer powder.

Keywords: peptoid; biomaterials; glass transition temperature; DSC; TGA; XRD

1. Introduction

At the beginning of the 20th century Leuchs [1–3] discovered by chance a synthesis of α -amino acid *N*-carboxy anhydrides (NCAs), also known as Leuchs anhydrides. Subsequently, this class of molecules would be applied for the ring-opening polymerization to obtain synthetic polypeptides.

Since the early 1950s many publications have dealt with mechanistic studies on the ring-opening polymerization of NCAs [4–11]. In the course of this, the class of N-substituted glycine *N*-carboxy anhydrides (NNCAs), represented solely by sarcosine-NCA (*N*-methylglycine-NCA), served predominantly to investigate the influence of amide proton on the polymerization. Other members of the resulting class of polymer (polypeptoids) were virtually unknown to polymer chemists until very recently. Sisido *et al.* only briefly mentioned poly(*n*-propylglycine) and poly(ethylglycine), without providing any characterization [12–14]. This limited interest in this polymer family may be attributed to an early report by Wessely *et al.*, in which it was suggested that NNCAs are exceedingly sensitive to hydrolysis [5].

In the meantime, Sisido *et al.* [15], Okada *et al.* [16] and Kricheldorf *et al.* [17] demonstrated that the polymerization of sarcosine-NCA could be controlled more readily as compared to regular amino acid NCAs. More recently, Zhang and co-workers found that N-substituted NCAs could be polymerized yielding cyclic polypeptoids with excellent yield in a well-controlled manner [18–21].

The living character of the nucleophilic ring-opening polymerization (NuLROP) of NNCAs other than Sar-NCA was shown by Luxenhofer and co-workers [22]. In particular, the successful preparation of a pentablock quinquepolymer highlighted the unique character of the NNCA NuLROP [23]. Moreover, efficient polymer analogue modification [24,25] and thermo-responsiveness [26,27] of polypeptoids was described.

The fact that polypeptoids can be prepared to yield highly defined linear or cyclic oligomer/polymers *via* step-wise solid phase synthesis or living ring-opening polymerization makes this class of polymer rather unique, as outlined in a recent review by Zhang *et al.* [28].

As this polymer class is rather new, little is known about the materials properties. Interestingly, Segalman studied a series of short sequence-specific polypeptoids (obtained by solid phase synthesis) in their crystallization and melting behavior [29]. As expected, melting points are lower than those of polypeptides (attributed to the lack of intermolecular H-bonding) and the crystallization behavior is strongly affected by the polymer side chain.

Here, we present a systematic study of the thermal stability, glass transition and melting points of polypeptoids bearing short (C_1 – C_5) side chains of degrees of polymerization of 10–100. X-Ray diffraction studies confirm that polysarcosine and poly(*N*-ethylglycine) are amorphous solids while longer side chain yield semicrystalline materials.

2. Experimental Section

2.1. Materials

All the solvents and substances for the preparation of monomers and polymers were purchased from Aldrich or Acros and were used as received unless otherwise stated. Benzonitrile (BN) was dried by refluxing over P_2O_5 , benzylamine over BaO and petrolether over CaH_2 under dry argon atmosphere and subsequent distillation prior to use. Water levels were determined using a C20 compact coulometer (Mettler-Toledo, Giessen, Germany). In general, solvents were used at water levels <30 ppm. The monomers were handled preferably in a glovebox (UNILab, MBraun, Garching, Germany).

2.2. Methods

Gel permeation chromatography (GPC) was performed on a PL-GPC-120 (Polymer Laboratories) running under WinGPC software (PSS, Mainz, Germany) with two consecutive Gram columns (100 and 1000 Å) with *N,N*-dimethylacetamide (DMAc) (5 g/L LiBr, 70 °C, 1 mL/min) as eluent and calibrated against PMMA standards (PSS, Mainz, Germany).

NMR spectra were recorded on a Bruker DRX 500 at room temperature (295 K). The spectra were calibrated using the solvent signals (D_2O 4.79 ppm, $\text{MeOD}-d_3$ 3.31 ppm, $\text{DMSO}-d_6$ 2.50, $\text{MeCN}-d_3$ 1.94 ppm).

Matrix assisted laser desorption/ionization time-of-flight (MALDI-ToF) mass spectra were recorded on a Bruker Biflex IV (Bruker Daltonics, Bremen, Germany) using a N_2 laser ($\lambda = 337$ nm). All spectra were recorded in positive reflector mode. The ions were accelerated using a potential of 19 kV and reflected using a voltage of 20 kV. Detection was typically set from 350 m/z to 10000 m/z with a matrix suppression of typically 350–1000 m/z. After parameter optimization for each measurement, the instrument was calibrated with Peptide Calibration Standard II and/or Oligonucleotide Calibration Standard (Bruker), depending on the m/z range of the individual sample. Samples were prepared with sinapinic acid (3,5-dimethoxy-4-hydroxycinnamic acid, SA) as matrix using the dried–droplet spotting technique (0.5–1 µL). Exemplarily, samples (1 g/L) were dissolved in methanol (supplemented with 1% (v/v) trifluoroacetic acid (TFA)). The solution was mixed 1:1 (v/v) with 20 g/L SA MeOH/1% TFA. Laser power was set slightly above the threshold, typically at 50%. Gauss distributions were calculated using Equation (1), where μ is the degree of polymerization (DP) obtained from the signal with highest intensity (M_p). The obtained probabilities are plotted against the calculated m/z at the respective DP and overlaid with the experimental MALDI-ToF mass spectra to estimate the molar mass (M_n , M_w) and the dispersity of the polymers (D_M).

$$f(x) = \frac{1}{\sigma\sqrt{2\pi}} e^{-\frac{1}{2}\left(\frac{x-\mu}{\sigma}\right)^2} \quad (1)$$

Thermogravimetric analysis was realized with a TG 50 modular unit and a TC 15 TA controller (Mettler-Toledo, Giessen, Germany).

DSC studies of the polypeptoids were conducted using a DSC 4 calorimeter (Perkin Elmer) under nitrogen. Powder samples sealed into the aluminum pans were first heated from 0 °C (except poly(*N*-butylglycine)₂₅ and poly(*N*-pentylglycine)₂₅ which started by -25 °C) to 250 °C at 5 K min⁻¹, depending on the decomposition temperature of the sample, cooled to 0 °C by use of air cooling (~24 K min⁻¹). Some additional measurements were conducted using a DSC 204 F1 Phoenix (Netzsch). Experimental data of glass transition temperature against the DP were fitted using Flory-Fox Equation (2).

$$T_g = T_g^\infty - A/M_n \quad (2)$$

With M_n as derived from ¹H-NMR and parameters listed in Table 1.

X-ray diffraction measurements were performed on the powder diffractometer Stadi P from STOE using the Cu-K α radiation wavelength ($\lambda = 1.54$ Å). Measuring range comprised 10 to 80 2θ.

Table 1. Parameters used Flory-Fox equation to obtain fits.

	A	T _g
PSar	71,000 K·g/mol	428 K
P(N-EtGly)	52,000 K·g/mol	396 K
P(N-PrGly)	69,000 K·g/mol	373 K
P(N-PenGly)	35,000 K·g/mol	283 K

2.3. Synthetic Procedures

2.3.1. Monomer Synthesis

Sarcosine-NCA:

Sarcosine-N-carboxyanhydride was synthesized in tetrahydrofuran (THF) in the presence of triphosgene as described previously [22].

N-Ethylglycine-, N-n-propylglycine-, N-n-butylglycine- and N-n-pentylglycine-NCA:

These monomers were obtained by a three-step synthesis from primary amines and glyoxylic acid using modified literature procedures [5,20] and was described previously [22,23].

2.3.2. Preparation of Polymers

Poly(sarcosine)₂₅ **P2**.

Sar-NCA (0.265 g, 2.3 mmol) was weighed into reaction vessel dissolved in 2.3 mL of dry benzonitrile. After complete dissolution, the initiator benzylamine (10.0 μ L, 0.09 mmol) was added ($[M]_0/[I]_0 = 25$). Outside of the glovebox the reaction mixture was stirred at room temperature under constant pressure (20 mbar) for 2 h. Afterwards, reaction mixture was precipitated into 40 mL diethyl ether and isolated polysarcosine was dried under reduced pressure. After two precipitation steps polysarcosine was dissolved in water and subsequently freeze-dried (0.135 g, 83%).

GPC (DMAc): $M_n = 1.3 \text{ kg/mol}$ ($D_M = M_w/M_n = 1.31$).

¹H NMR (500 MHz; D₂O): $\delta = 2.97$ (66 H, br, CH₃–), 4.29 (46 H, br, –CH₂–CO– and C₆H₅–CH₂–NH–), 7.35 ppm (5 H, br, C₆H₅–).

All other polymers were synthesized accordingly.

Poly(sarcosine)₁₀ **P1**.

¹H NMR (500 MHz; D₂O): $\delta = 2.99$ (23 H, br, CH₃–), 4.28 (17 H, br, –CH₂–CO– and C₆H₅–CH₂–NH–), 7.33 ppm (5 H, br, C₆H₅–).

Poly(sarcosine)₅₀ **P3**.

GPC (DMAc): $M_n = 4.0 \text{ kg/mol}$ ($D_M = M_w/M_n = 1.09$).

¹H NMR (500 MHz; D₂O): $\delta = 2.96$ (135 H, br, CH₃–), 4.28 (90 H, br, –CH₂–CO– and C₆H₅–CH₂–NH–), 7.32 ppm (5 H, br, C₆H₅–).

Poly(sarcosine)₁₀₀ **P4**.

GPC (DMAc): $M_n = 8.9 \text{ kg/mol}$ ($D_M = M_w/M_n = 1.05$).

¹H NMR (500 MHz; D₂O): $\delta = 2.95$ (219 H, br, CH₃–), 4.28 (146 H, br, –CH₂–CO– and C₆H₅–CH₂–NH–), 7.33 ppm (5 H, br, C₆H₅–).

Poly(N-ethylglycine)₁₀ **P5**.

¹H NMR (500 MHz; D₂O): δ = 1.14 (32 H, br, CH₃–), 3.37 (19 H, br, CH₃–CH₂–), 4.25 (23 H, br, –CH₂–CO– and C₆H₅–CH₂–NH–), 7.32 ppm (5 H, br, C₆H₅–).

Poly(*N*-ethylglycine)₂₅ **P6**.

GPC (DMAc): M_n = 1.0 kg/mol (D_M = M_w/M_n = 1.65).

¹H NMR (500 MHz; D₂O): δ = 1.14 (70 H, br, CH₃–), 3.38 (45 H, br, CH₃–CH₂–), 4.26 (48 H, br, –CH₂–CO– and C₆H₅–CH₂–NH–), 7.32 ppm (5 H, br, C₆H₅–).

Poly(*N*-ethylglycine)₅₀ **P7**.

GPC (DMAc): M_n = 3.3 kg/mol (D_M = M_w/M_n = 1.27).

¹H NMR (500 MHz; D₂O): δ = 1.14 (116 H, br, CH₃–), 3.38 (73 H, br, CH₃–CH₂–), 4.22 (74 H, br, –CH₂–CO– and C₆H₅–CH₂–NH–), 7.32 ppm (5 H, br, C₆H₅–).

Poly(*N*-ethylglycine)₁₀₀ **P8**.

GPC (DMAc): M_n = 6.8 kg/mol (D_M = M_w/M_n = 1.22).

¹H NMR (500 MHz; D₂O): δ = 1.14 (252 H, br, CH₃–), 3.38 (164 H, br, CH₃–CH₂–), 4.25 (170 H, br, –CH₂–CO– and C₆H₅–CH₂–NH–), 7.32 ppm (5 H, br, C₆H₅–).

Poly(*N*ⁿ-propylglycine)₁₀ **P9**.

GPC (DMAc): M_n = 0.6 kg/mol (D_M = M_w/M_n = 1.58).

¹H NMR (500 MHz; MeOD-*d*₃): δ = 0.92 (38 H, br, CH₃–), 1.60 (25 H, br, CH₃–CH₂–), 3.33 (n.d., br, CH₃–CH₂–CH₂–), 4.25 (25 H, br, –CH₂–CO– and C₆H₅–CH–NH–), 7.25 ppm (5 H, br, C₆H₅–).

Poly(*N*ⁿ-propylglycine)₂₅ **P10**.

GPC (DMAc): M_n = 1.6 kg/mol (D_M = M_w/M_n = 1.32).

¹H NMR (500 MHz; MeOD-*d*₃): δ = 0.92 (66 H, br, CH₃–), 1.60 (45 H, br, CH₃–CH₂–), 3.32 (n.d., br, CH₃–CH₂–CH₂–), 4.25 (43 H, br, –CH₂–CO– and C₆H₅–CH₂–NH–), 7.25 ppm (5 H, br, C₆H₅–).

Poly(*N*ⁿ-propylglycine)₅₀ **P11**.

GPC (DMAc): M_n = 5.0 kg/mol (D_M = M_w/M_n = 1.22).

¹H NMR (500 MHz; MeCN-*d*₃): δ = 0.86 (50 H, br, CH₃–), 1.52 (37 H, br, CH₃–CH₂–), 3.23 (32 H, br, CH₃–CH₂–CH₂–), 4.10 (39 H, br, –CH₂–CO– and C₆H₅–CH₂–NH–), 7.28 ppm (5 H, br, C₆H₅–).

Poly(*N*ⁿ-propylglycine)₁₀₀ **P12**.

GPC (DMAc): M_n = 7.5 kg/mol (D_M = M_w/M_n = 1.15).

¹H NMR (500 MHz; MeOD-*d*₃): δ = 0.92 (222 H, br, CH₃–), 1.62 (149 H, br, CH₃–CH₂–), 3.33 (n.d., br, CH₃–CH₂–CH₂–), 4.27 (146 H, br, –CH₂–CO– and C₆H₅–CH₂–NH–), 7.26 ppm (5 H, br, C₆H₅–).

Poly(*N*ⁿ-butylglycine)₁₀ **P13**.

GPC (DMAc): M_n = 0.9 kg/mol (D_M = M_w/M_n = 1.55).

¹H NMR (500 MHz; TFA (DMSO-*d*₆)): δ = 0.87 (33 H, br, CH₃–), 1.30 (23 H, br, CH₃–CH₂–), 1.61 (22 H, br, CH₃–CH₂–CH₂–), 3.33 (22 H, br, CH₃–(CH₂)₂–CH₂–), 4.38 (25 H, br, –CH₂–CO– and C₆H₅–CH₂–NH–), 7.17 ppm (5 H, br, C₆H₅–).

Poly(*N*ⁿ-butylglycine)₂₅ **P14**.

GPC (DMAc): M_n = 1.9 kg/mol (D_M = M_w/M_n = 1.27).

¹H NMR (500 MHz; TFA (DMSO-*d*₆)): δ = 0.86 (60 H, br, CH₃–), 1.43 (82 H, br, CH₃–CH₂–CH₂–), 3.34 (40 H, br, CH₃–(CH₂)₂–CH₂–), 4.32 (39 H, br, –CH₂–CO– and C₆H₅–CH₂–NH–), 7.16 ppm (5 H, br, C₆H₅–).

Poly(*N*ⁿ-butylglycine)₅₀ **P15**.

GPC (DMAc): M_n = 3.2 kg/mol (D_M = M_w/M_n = 1.40).

¹H NMR (500 MHz; TFA (DMSO-*d*₆)): δ = 0.87 (113 H, br, CH₃–), 1.31 (77 H, br, CH₃–CH₂–), 1.62 (75 H, br, CH₃–CH₂–CH₂–), 3.36 (76 H, br, CH₃–(CH₂)₂–CH₂–), 4.39 (80 H, br, –CH₂–CO– and C₆H₅–CH₂–NH–), 7.16 ppm (5 H, br, C₆H₅–).

Poly(*N*ⁿbutylglycine)₁₀₀ **P16**.

GPC (DMAc): M_n = 4.2 kg/mol (D_M = M_w/M_n = 1.16).

¹H NMR (500 MHz; TFA (DMSO-*d*₆)): δ = 0.87 (172 H, br, CH₃–), 1.30 (122 H, br, CH₃–CH₂–), 1.62 (115 H, br, CH₃–CH₂–CH₂–), 3.36 (117 H, br, CH₃–(CH₂)₂–CH₂–), 4.34 (125 H, br, –CH₂–CO– and C₆H₅–CH₂–NH–), 7.16 ppm (5 H, br, C₆H₅–).

Poly(*N*ⁿpentylglycine)₁₀ **P17**.

GPC (DMAc): M_n = 0.9 kg/mol (D_M = M_w/M_n = 1.38).

¹H NMR (500 MHz; TFA (DMSO-*d*₆)): δ = 0.82 (30 H, br, CH₃–), 1.27 (41 H, br, CH₃–CH₂–CH₂–), 1.64 H (20 H, br, CH₃–(CH₂)₂–CH₂–), 3.35 (20 H, br, CH₃–(CH₂)₃–CH₂–), 4.39 (25 H, br, –CH₂–CO– and C₆H₅–CH₂–NH–), 7.16 ppm (5 H, br, C₆H₅–).

Poly(*N*ⁿpentylglycine)₂₅ **P18**.

GPC (DMAc): M_n = 2.1 kg/mol (D_M = M_w/M_n = 1.20).

¹H NMR (500 MHz; TFA (DMSO-*d*₆)): δ = 0.83 (51 H, br, CH₃–), 1.27 (67 H, br, CH₃–CH₂–CH₂–), 1.64 (34 H, br, CH₃–(CH₂)₂–CH₂–), 3.33 (34 H, br, CH₃–(CH₂)₃–CH₂–), 4.45 (36 H, br, –CH₂–CO– and C₆H₅–CH₂–NH–), 7.16 ppm (5 H, br, C₆H₅–).

Poly(*N*ⁿpentylglycine)₅₀ **P19**.

¹H NMR (500 MHz; TFA (DMSO-*d*₆)): δ = 0.82 (111 H, br, CH₃–), 1.27 (149 H, br, CH₃–CH₂–CH₂–), 1.65 (73 H, br, CH₃–(CH₂)₂–CH₂–), 3.36 (75 H, br, CH₃–(CH₂)₃–CH₂–), 4.45 (79 H, br, CH₂–CO– and C₆H₅–CH₂–NH–), 7.16 ppm (5 H, br, C₆H₅–).

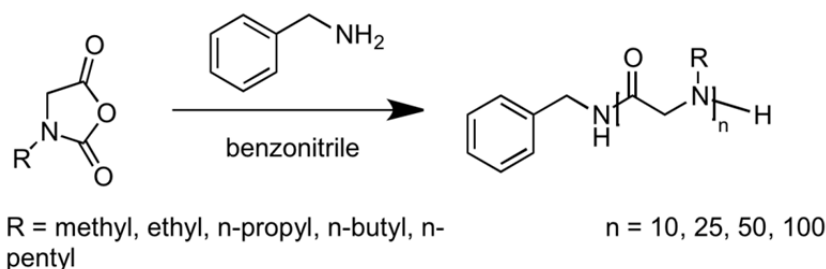
Poly(*N*ⁿpentylglycine)₁₀₀ **P20**.

¹H NMR (500 MHz; TFA (DMSO-*d*₆)): δ = 0.82 (190 H, br, CH₃–), 1.27 (258 H, br, CH₃–CH₂–CH₂–), 1.65 (127 H, br, CH₃–(CH₂)₂–CH₂–), 3.36 (130 H, br, CH₃–(CH₂)₃–CH₂–), 4.45 (140 H, br, CH₂–CO– and C₆H₅–CH₂–NH–), 7.16 ppm (5 H, br, C₆H₅–).

3. Results and Discussion

Polypeptoids with different degrees of polymerization (DP) and varying side-chain length comprising 1 to 5 carbon atoms were successfully synthesized (Scheme 1).

Scheme 1. Schematic representation of synthesis of homo polypeptoids prepared in this work.



Characterization of the obtained polypeptoids was performed using ^1H NMR spectroscopy, GPC and MALDI-ToF mass spectrometry (Table 2). The polymers **P19** and **P20** (poly(*N*-pentylglycine)) were insoluble in the used solvents (DMAc, MeOH), therefore the characterization by GPC and MALDI-ToF MS was not possible. Furthermore, the molar mass of **P1** and **P5** was too small for the GPC measurement under the given conditions.

Table 2. Analytical data of synthesized polypeptoids.

Polymer ^a	M_n ^b [kg/mol]	\overline{D}_M ^b	M_n ^c [kg/mol]	\overline{D}_M ^c	M_n ^d [kg/mol]	DP ^d	yield [%]
P1	PSar ₁₀	-	0.7	1.06	0.6 ^e	7 ^e	65
P2	PSar ₂₅	1.3	1.31	1.6	1.08	1.7 ^e	22 ^e
P3	PSar ₅₀	4.0	1.09	3.5	1.01	3.8 ^e	52 ^e
P4	PSar ₁₀₀	8.9	1.05	7.2	1.01	5.3 ^e	73 ^e
P5	P(<i>N</i> -EtGly) ₁₀	-	1.0	1.06	1.0 ^e	10.5 ^e	-
P6	P(<i>N</i> -EtGly) ₂₅	1.0	1.65	2.0	1.05	2.1 ^e	23 ^e
P7	P(<i>N</i> -EtGly) ₅₀	3.3	1.25	3.3	1.06	3.9 ^e	45 ^e
P8	P(<i>N</i> -EtGly) ₁₀₀	6.8	1.22	6.6	1.01	7.2 ^e	83 ^e
P9	P(<i>N</i> -PrGly) ₁₀	0.6	1.58	1.4	1.03	1.4 ^f	13 ^f
P10	P(<i>N</i> -PrGly) ₂₅	1.6	1.32	2.0	1.04	2.3 ^f	22 ^f
P11	P(<i>N</i> -PrGly) ₅₀	5.0	1.22	4.2	1.04	4.1 ^g	40 ^g
P12	P(<i>N</i> -PrGly) ₁₀₀	7.5	1.15	6.0	1.03	7.4 ^f	74 ^f
P13	P(<i>N</i> -BuGly) ₁₀	0.9	1.55	1.4	1.06	1.4 ^h	11 ^h
P14	P(<i>N</i> -BuGly) ₂₅	1.9	1.27	1.9	1.16	2.2 ^h	18.5 ^h
P15	P(<i>N</i> -BuGly) ₅₀	3.2	1.40	4.4	1.04	4.4 ^h	38 ^h
P16	P(<i>N</i> -BuGly) ₁₀₀	4.2	1.16	-	-	6.8 ^h	59 ^h
P17	P(<i>N</i> -PenGly) ₁₀	0.9	1.38	1.4	1.03	1.5 ^h	11 ^h
P18	P(<i>N</i> -PenGly) ₂₅	2.1	1.2	1.9	1.16	2.3 ^h	17 ^h
P19	P(<i>N</i> -PenGly) ₅₀	-	-	-	-	4.9 ^h	38 ^h
P20	P(<i>N</i> -PenGly) ₁₀₀	-	-	-	-	8.4 ^h	65 ^h
							>99 ⁱ

^a As determined from $[M]_0/[I]_0$; ^b As determined by gel permeation chromatography; ^c As calculated from Gauss distribution fitted to MALDI-ToF mass spectra; ^d As determined by end-group analysis from ^1H NMR spectroscopy (signal intensity of aromatic protons of benzylamine-initiator vs main-chain and side-chain signal intensity); ^e Determined in D_2O ; ^f Determined in MeOD ; ^g Determined in MeCN ; ^h Determined in $\text{TFA}-d_7$ with $\text{DMSO}-d_6$ as external lock; ⁱ Traces of solvents could be contained in the polymers.

A comparison of the obtained molar masses with the theoretical masses calculated from $[M]_0/[I]_0$ using the example of P(*N*-PrGly) with different degrees of polymerization shows an increasing discrepancy with an increasing DP (Figure 1). This has been reported before by others and us [17,22,25]. To date, we lack a satisfactory explanation. Nevertheless, the experimentally determined degrees of polymerization generally follow the expected trend.

The thermal properties of the different polypeptoids have been investigated by thermogravimetric analysis (TGA) and differential scanning calorimetry (DSC) (Table 3).

Figure 1. Correlation of the determined molar mass (by GPC, MALDI-ToF and ^1H NMR spectroscopy, respectively) of different poly(*N*-propylglycine) (P(*N*-PrGly)) with the theoretical molar mass.

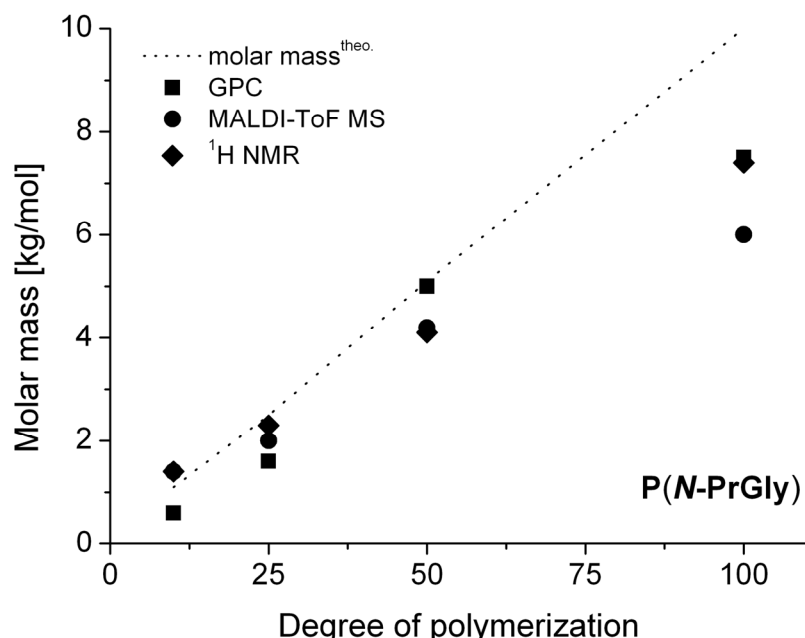


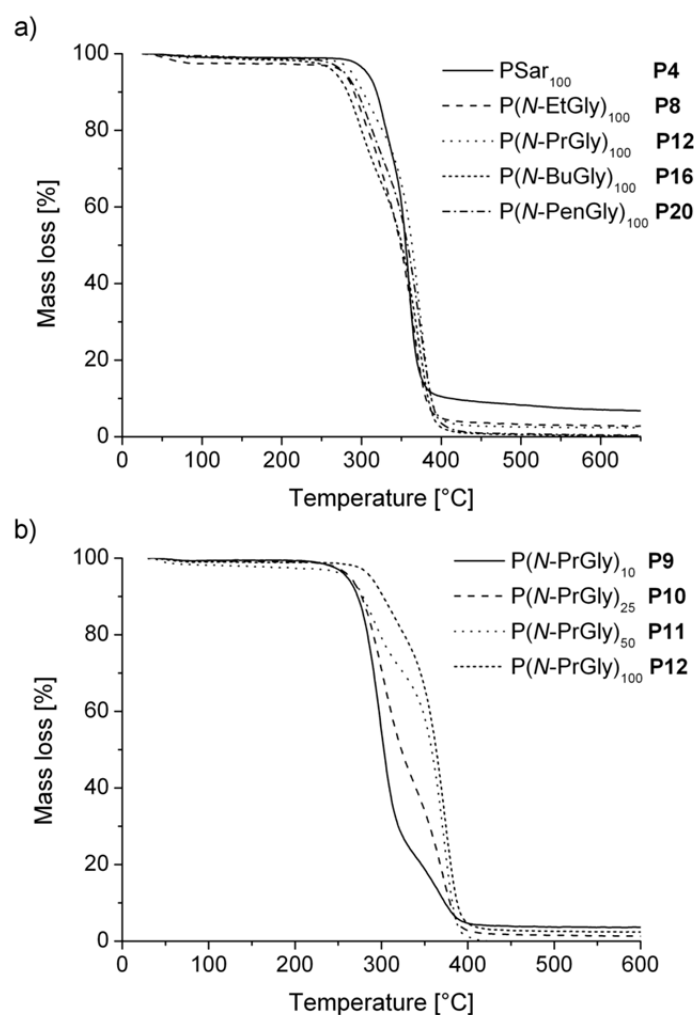
Table 3. Summary of the DSC and TGA studies.

polymer ^a	T _g [°C]	T _m [°C]	T _c [°C] ^b	T _d [°C] ^c
P1	PSar ₁₀	28	-	175
P2	PSar ₂₅	127	-	210
P3	PSar ₅₀	136	-	215
P4	PSar ₁₀₀	143	-	250
P5	P(<i>N</i> -EtGly) ₁₀	77	-	n.d.
P6	P(<i>N</i> -EtGly) ₂₅	93	-	220
P7	P(<i>N</i> -EtGly) ₅₀	107	-	215
P8	P(<i>N</i> -EtGly) ₁₀₀	114	-	240
P9	P(<i>N</i> -PrGly) ₁₀	34	-	205
P10	P(<i>N</i> -PrGly) ₂₅	66	163	210
P11	P(<i>N</i> -PrGly) ₅₀	88	190	150
P12	P(<i>N</i> -PrGly) ₁₀₀	93	198	166
P13	P(<i>N</i> -BuGly) ₁₀	-	153	210
P14	P(<i>N</i> -BuGly) ₂₅	4	173	n.d.
P15	P(<i>N</i> -BuGly) ₅₀	-	215 (2 nd T _m = 63 °C)	215
P16	P(<i>N</i> -BuGly) ₁₀₀	-	225 (2 nd T _m = 70 °C)	213
P17	P(<i>N</i> -PenGly) ₁₀	-	145 (2 nd T _m = 56 °C)	205
P18	P(<i>N</i> -PenGly) ₂₅	-3	176 (2 nd T _m = 49 °C)	n.d.
P19	P(<i>N</i> -PenGly) ₅₀	1	190 (2 nd T _m = 70 °C)	220
P20	P(<i>N</i> -PenGly) ₁₀₀	5	207 (2 nd T _m = 67 °C)	220

^a As determined from $[M]_0/[I]_0$; ^b crystallization temperature; ^c decomposition temperature.

The TGA thermograms of all polypeptoid samples, except **P1**, reveal decomposition temperature thresholds over 200 °C, which is in accordance with earlier reports for several other polypeptoids with long-chain substituents [29]. In Figure 2, an assortment of TGA thermograms is displayed. On the one hand, polypeptoid samples with an increasing side chain length were compared (Figure 2a), on the other hand the influence of the DP based on different P(*N*-PrGly) samples is depicted (Figure 2b). The influence of the substituent on the decomposition temperature is relatively little; in contrast, with an increasing DP, a shift to higher decomposition temperatures is noticeable.

Figure 2. Comparison of TGA thermograms of different polypeptoid samples with (a) an increase in side chain length and (b) different degrees of polymerization.

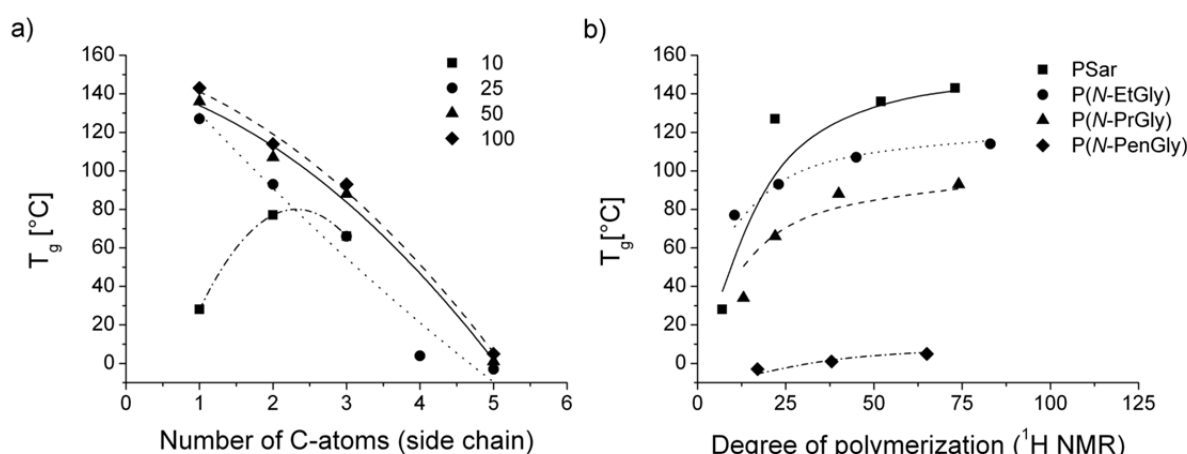


The decomposition temperature of polysarcosine is comparable with the sarcosine decomposition temperature of 212.5 °C. To the best of our knowledge, no decomposition temperatures have been published for the other corresponding N-substituted glycines.

Rosales *et al.* reported that poly(*N*-isopentylglycine), poly(*N*-hexylglycine) and other polypeptoids with longer side chains were stable up to 260 °C. In our case, the on-set temperatures were significantly lower than 260 °C. Unfortunately, a more detailed comparison with literature is not possible as no detailed decomposition values or thermograms were given [29].

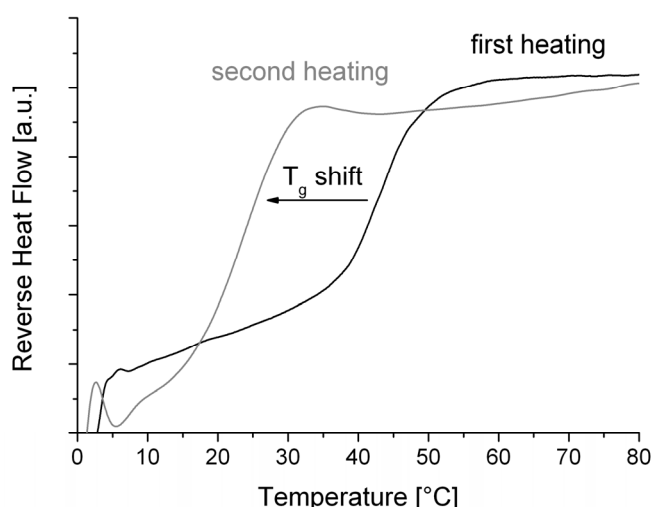
DSC studies were carried out below the decomposition temperatures to determine glass transition temperature (T_g) and melting points (T_m). The glass transition temperature as a function of the number of C-atoms in the side chain and of different degrees of polymerization was investigated (Figure 3). Different polypeptoid samples with the same DP, but increasing number of C-atoms in the side chain possess, as expected, decreasing glass transition temperatures (Figure 3a). Comparison of the T_g 's of **P4** ($T_g = 143$ °C) and **P20** ($T_g = 5$ °C) exhibit a difference of 138 °C. In the literature a $T_g = 117$ °C for polysarcosine with a DP of 103 can be found [30].

Figure 3. Depiction of the glass transition temperature (T_g) as a function (a) of number of C-atoms in the side chain at different degrees of polymerization and (b) of the DP. Please note, lines in (a) represent only a guide for the eye. Lines in (b) are derived from Flory-Fox equation ($T_g = T_g^\infty - A/M_n$) as outlined in experimental part.



Notably, the T_g value of **P1** does not fit in the observed trend. This may be attributed in part to the low decomposition on-set temperature. Possibly, the decomposition of the polymer starts in the first heating cycle, the consequence being that the glass transition was drastically decreased (Figure 4). However, the determined T_g from the first heating cycle is already very low.

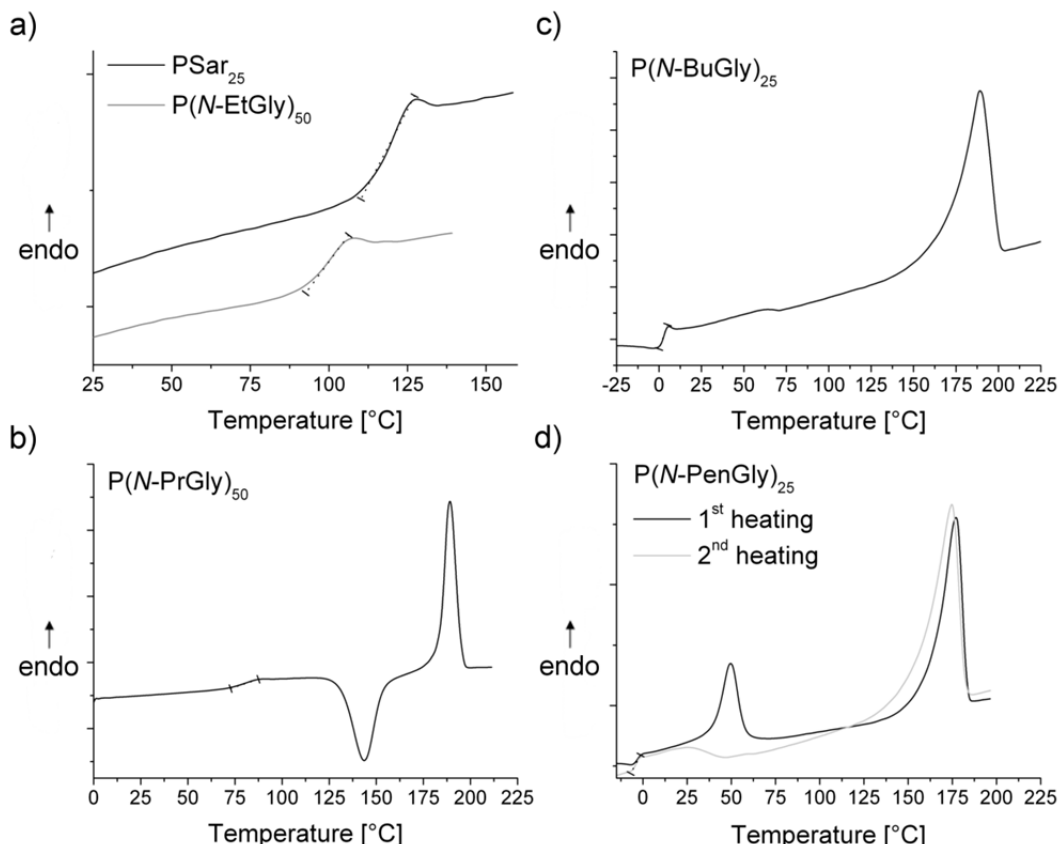
Figure 4. Shift of the glass transition temperature of **P1** after the first heating cycle.



The decrease of the T_g by increasing side chain length is associated with extended flexibility of the backbone. Such decrease is expected and has also been studied in some detail for poly(2-oxazoline)s, constitutional isomers of polypeptoids [31]. Moreover, another trend is recognizable in Figure 3b. As is well known, an increase of the DP leads to an increase of the T_g [32,33]. An increase of the chain length decreases the flexibility of the polymer chains, the consequence being that the T_g increase to a constant value. In addition, the chain ends may act as plasticizers [34]. As the relative amount of polymer chain ends decreases with increase in chain length, the T_g reaches a plateau. For PSar, P(*N*-EtGly) and P(*N*-PrGly) this plateau appears to be reached at approx. DP = 50.

It should be noted that for unknown reasons P(*N*-BuGly) did not yield values for T_g for DPs other than 25 in this study. We are currently investigating this issue in more detail, as it may be that small residual of solvent is responsible for this. Some DSC response curves are depicted in Figure 5. We observed melting points for polypeptoids with a side chain comprising not less than three methyl carbon atoms. That implies that PSar and P(*N*-EtGly) are amorphous solids. Our data corroborates earlier reports by Okada *et al.* [30]. However, P(*N*-PrGly), P(*N*-BuGly) P(*N*-BuGly) and exhibit crystalline domains in the solid structure.

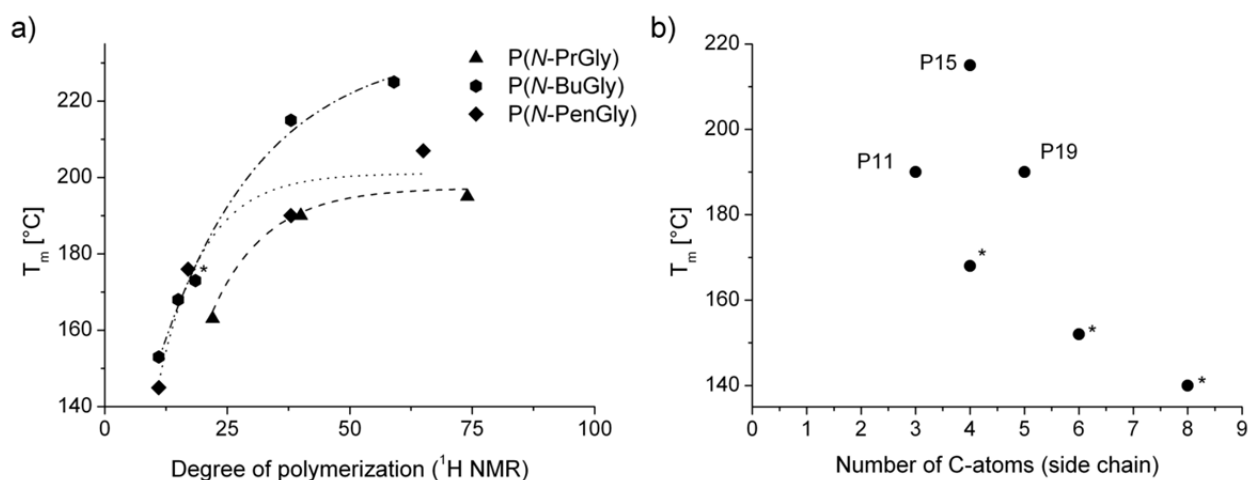
Figure 5. (a), (b), (c) Second heating DSC thermograms of some synthesized polypeptoids and **(d)** comparison of the first and second heating DSC thermogram of P(*N*-PenGly)₂₅ (**P18**). Glass transition temperature ranges were marked with a dotted line in each thermogram.



The obtained values for T_m of the polypeptoids follow the same trend as the glass transition temperature, *i.e.*, with increasing chain length the T_m increases towards a plateau (Figure 6a).

Interestingly, polymer T_m values at a fixed DP are highest for the P(*N*-BuGly). The value we report here for P(*N*-BuGly) again corroborate and supplement values reported by Rosales *et al.* Moreover, T_m values for P(*N*-PenGly) align roughly with literature values for poly(*N*-hexylglycine) and poly(*N*-octylglycine), although it must be noted that for those samples, a the smaller DP of 15 was reported (Figure 6b) [29]. In addition, these samples were monodisperses.

Figure 6. Comparison of polymer melting temperatures (T_m) as a function of (a) the degree of polymerization and (b) the polymer side chain length. Please note, values marked with asterisks were obtained by graphical extraction from ref.[29] and represent polymers with a degree of polymerization of 15. Lines in (a) only serve as guide for the eyes.



The first and second heating DSC thermogram of P(*N*-PenGly)₂₅ (**P18**) are shown in Figure 5d). The first heating thermogram exhibits two signals (in the range of 50 °C and 175 °C) which can be assigned to melting points. Interestingly, while for the other degrees of polymerization (**P17**, **P19**, **P20**) the lower temperature T_m persists in the second heating cycle no signal was detected at 50 °C therein for **P18**. In lieu thereof a buckle in the curve can be observed. Zhang *et al.* observed two melting points for the polypeptoid with a decyl substituent at the nitrogen and attributed this phenomenon to crystalline packing of the side chains and the main chains [35]. Accordingly, we also attribute the observed signals to crystalline packing of the side chains, but after the cooling cycle no melting point is observed in the second heating cycle. Repetition of the measurement revealed clearly smaller signals for the melting point in the range of 50 °C (data not shown). However, the melting point existed in the second heating curve as well.

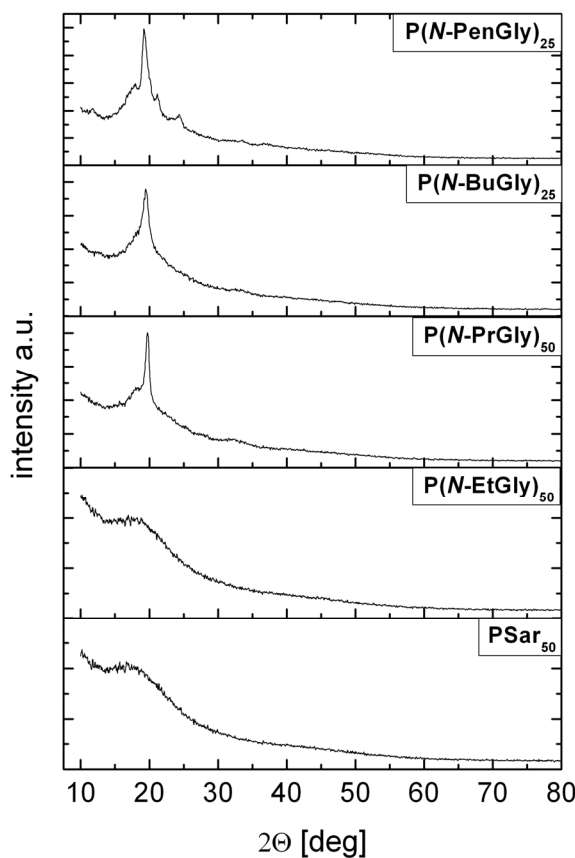
The DSC thermogram of P(*N*-PrGly) shows an exothermic peak in the range of 143–155 °C, which can indicates a cold-crystallization process (Figure 5b). This peak describes the transition from amorphous solid to crystalline solid.

It should be noted that we observed a number of problems with repeatability of DSC measurements for some samples. In a number of cases, it appears that decomposition/discoloration started briefly after the glass transition temperature although TGA thermograms give no indication of a change in sample mass. The presence of flat and/or asymmetric peaks, decreasing T_g and T_m and discoloring of the samples after the measurement (yellow-brown), do hint towards changes in the polymer structure during these measurements. As may be expected, the problem with DSC measurement reproducibility

was particularly pronounced for samples of low molar mass. We attribute this to more pronounced end-group effects for short polymer chains.

Crystallinity of polymer powders was also assessed using X-ray diffraction (Figure 7). Diffractograms of PSar and P(N-EtGly) show no sharp signals. This observation corresponds to amorphous solids and corroborates the observed lack of melting points by DSC. In contrast the diffractograms of the other three polymers (P(N-PrGly) (**P11**), P(N-BuGly) (**P14**) and P(N-PenGly) (**P18**) exhibit a sharp signal in a range of 20° – 2θ , which is evidence for crystalline domains in the polymer powder. Rosales *et al.* detected a reflection in this range for all investigated peptoids and attributed this observation to the spacing between polymer chains ($d = 4.5 \text{ \AA}$) based on previously investigations [29,36]. Furthermore, P(N-PenGly) exhibits a reflection in the range of 25° – 2θ . Zhang *et al.* investigated cyclic poly(*N*-decylglycine) with WAXS and attributed a reflection in the same range to the distance between adjacent repeating units ($d = 3.6 \text{ \AA}$) [35].

Figure 7. Powder XRD diffractograms of some synthesized polypeptoids.



4. Conclusions

We have investigated a series of polypeptoid homopolymers bearing short (C_1 – C_5) side chains of DP = 10–100 regarding thermal stability, glass transition and melting points. First, we synthesized polypeptoids by nucleophilic living ring-opening polymerization and characterized the obtained polymers with ^1H NMR spectroscopy, MALDI-ToF mass spectrometry and gel permeation chromatography. Afterwards, thermal properties of the different polypeptoids have been investigated by thermogravimetric analysis (TGA) and differential scanning calorimetry. TGA thermograms reveal

decomposition temperature thresholds over 200 °C. Side chain length and DP affect the decomposition temperatures differently. The influence of the side chain is relatively little. However, an increasing DP leads to a shift to higher decomposition temperatures.

Furthermore, dependences of the glass transition temperature were investigated regarding side chain length and degree of polymerization. The obtained values confirm expected trends for T_g values and corroborate values reported earlier where available. In summary, an increasing side chain length leads to a decrease the T_g while an increase of the DP increases the T_g to a constant value. Similar observations occurred for the melting points, *i.e.*, melting points increase to a constant value by increasing DP. However, three carbon atoms in the side chain are necessary to obtain semi-crystalline materials. Moreover, poly(*N*-butylglycine) and poly(*N*-pentylglycine) of degrees of polymerization of 50–100 exhibit two melting points which are attributed to crystalline packing of the side chains and the main chains.

X-ray diffraction measurements confirm crystalline domains in the polymer powder for polypeptoids with more than two carbon atoms in the side chain.

Acknowledgments

This publication is based on work supported by Award No. KUK-F1-029-32, made by King Abdullah University of Science and Technology (KAUST) and the Fonds der Chemischen Industrie (awarded to R.L.). We would like to acknowledge technical support by Matthias Kluge (TU Dresden) for TGA and DSC measurements. We kindly acknowledge technical support with XRD measurements by Anja Bensch (Prof. Michael Ruck, Inorganic Chemistry II at TU Dresden). The authors thank Julian Wagenhöfer for helpful discussions about XRD diffractograms. We also acknowledge Prof. Rainer Jordan (TU Dresden) for support and access to equipment. This publication was funded by the German Research Foundation (DFG) and the University of Wuerzburg in the funding programme Open Access Publishing.

References

1. Leuchs, H.; Geiger, W. Über die Anhydride von α -Amino-N-Carbonsäuren und die von α -Aminosäuren. *Chem. Ber.* **1908**, *41*, 1721–1726.
2. Leuchs, H.; Manasse, W. Über die Isomerie der Carbäthoxyl-glycyl glycinester. *Chem. Ber.* **1907**, *40*, 3235–3249.
3. Leuchs, H. Über die Glycin-Carbonsäure. *Chem. Ber.* **1906**, *39*, 857–861.
4. Sigmund, F.; Wessely, F. Untersuchungen über α -Amino-N-Carbonsäureanhydride. II. *H-S Z. Physiol. Chem.* **1926**, *157*, 91–105.
5. Wessely, F.; Riedl, K.; Tuppy, H. Untersuchungen über alpha-Amino-N-Carbonsäureanhydride VI. *Monatsh. Chem.* **1950**, *81*, 861–872.
6. Waley, S.G.; Watson, J. The Kinetics of the Polymerization of Sarcosine Carbonic Anhydride. *P. Roy. Soc. Lond. A Mat.* **1949**, *199*, 499–517.
7. Bamford, C.H.; Block, H.; Pugh, A.C. P. The polymerization of 3-substituted oxazolidine-2,5-diones. *J. Chem. Soc.* **1961**, *1961*, 2057–2063.

8. Hanby, W.E.; Waley, S.G.; Watson, J. Synthetic Polypeptides. Part I. *J. Chem. Soc.* **1950**, 3009–3013.
9. Ballard, D.G.; Bamford, C.H. Kinetics of the Formation of Polypeptides from N-Carboxy- α -amino-acid Anhydrides. *Nature* **1953**, 4365, 907–908.
10. Ballard, D.G.H.; Bamford, C.H. Studies in polymerization. X. “The chain-effect”. *P. Roy. Soc. Lond. A Mat.* **1956**, 236, 384–396.
11. Hadjichristidis, N.; Iatrou, H.; Pitsikalis, M.; Sakellariou, G. Synthesis of well-defined polypeptide-based materials via the ring-opening polymerization of alpha-amino acid N-carboxyanhydrides. *Chem. Rev.* **2009**, 109, 5528–5578.
12. Sisido, M.; Imanishi, Y.; Okamura, S. Polymerization of DL-beta-Phenylalanine N-Carboxyanhydride by Poly(*N*-n-Propylglycine) Diethylamide. *Polym. J.* **1970**, 1, 198–203.
13. Sisido, M.; Imanishi, Y.; Okamura, S. Polymerization of amino acid derivatives by polymer catalysts. V. Polymerization of DL- β -phenylalanine N-carboxyanhydride by several poly(*N*-alkylamino acid) diethylamides. *Biopolymers* **1970**, 9, 791–797.
14. Sisido, M.; Imanishi, Y.; Okamura, S. Polymerization of amino acid derivatives by polymer catalysts. III. Chain effect polymerization induced by poly(*N*-ethylglycine) diethylamide. *Biopolymers* **1969**, 7, 937–947.
15. Sisido, M.; Imanishi, Y.; Higashimura, T. Molecular weight distribution of polysarcosine obtained by NCA polymerization. *Makromol. Chem.* **1977**, 178, 3107–3114.
16. Aoi, K.; Hatanaka, T.; Tsutsumiuchi, K.; Okada, M.; Imae, T. Synthesis of a novel star-shaped dendrimer by radial-growth polymerization of sarcosine N-carboxyanhydride initiated with poly(trimethyleneimine) dendrimer. *Macromol. Rapid Commun.* **1999**, 20, 378–382.
17. Kricheldorf, H.R.; von Lossow, C.; Schwarz, G. Primary Amine-Initiated Polymerizations of Alanine-NCA and Sarcosine-NCA. *Macromol. Chem. Phys.* **2004**, 205, 918–924.
18. Tanisaka, H.; Kizaka-Kondoh, S.; Makino, A.; Tanaka, S.; Hiraoka, M.; Kimura, S. Near-infrared fluorescent labeled peptosome for application to cancer imaging. *Bioconjug. Chem.* **2008**, 19, 109–117.
19. Makino, A.; Kizaka-Kondoh, S.; Yamahara, R.; Hara, I.; Kanzaki, T.; Ozeki, E.; Hiraoka, M.; Kimura, S. Near-infrared fluorescence tumor imaging using nanocarrier composed of poly(L-lactic acid)-block-poly(sarcosine) amphiphilic polydepsipeptide. *Biomaterials* **2009**, 30, 5156–5160.
20. Guo, L.; Zhang, D. Cyclic poly(alpha-peptoid)s and their block copolymers from N-heterocyclic carbene-mediated ring-opening polymerizations of N-substituted N-carboxylanhydrides. *J. Am. Chem. Soc.* **2009**, 131, 18072–18074.
21. Guo, L.; Li, J.; Brown, Z.; Ghale, K.; Zhang, D. Synthesis and Characterization of Cyclic and Linear Helical Poly(alpha-peptoid)s by N-Heterocyclic Carbene-Mediated Ring-Opening Polymerizations of N-Substituted N-Carboxyanhydrides. *Biopolymers* **2011**, 96, 596–603.
22. Fetsch, C.; Grossmann, A.; Holz, L.; Nawroth, J.F.; Luxenhofer, R. Polypeptoids from N-Substituted Glycine N-Carboxyanhydrides: Hydrophilic, Hydrophobic, and Amphiphilic Polymers with Poisson Distribution. *Macromolecules* **2011**, 44, 6746–6758.
23. Fetsch, C.; Luxenhofer, R. Highly Defined Polypeptoids via Multiple Chain Extension and Macroinitiators. *Macromol. Rapid. Commun.* **2012**, 33, 1708–1713.

24. Lahasky, S.H.; Serem, W.K.; Guo, L.; Garno, J.C.; Zhang, D. Synthesis and Characterization of Cyclic Brush-Like Polymers by N-Heterocyclic Carbene-Mediated Zwitterionic Polymerization of N-Propargyl N-Carboxyanhydride and the Grafting-to Approach. *Macromolecules* **2011**, *44*, 9063–9074.
25. Robinson, J.W.; Schlaad, H. A versatile polypeptoid platform based on N-allyl glycine. *Chem. Commun.* **2012**, *48*, 7835–7837.
26. Lahasky, S.H.; Hu, X.; Zhang, D. Thermoresponsive Poly(α -peptoid)s: Tuning the Cloud Point Temperatures by Composition and Architecture. *ACS Macro Lett.* **2012**, *1*, 580–584.
27. Robinson, J.W.; Secker, C.; Weidner, S.; Schlaad, H. Thermo-responsive Poly(N-C₃ glycine)s. *Macromolecules* **2013**, *47*, in print.
28. Zhang, D.; Lahasky, S.H.; Guo, L.; Lee, C.-U.; Lavan, M. Polypeptoid Materials: Current Status and Future Perspectives. *Macromolecules* **2012**, *45*, 5833–5841.
29. Rosales, A.M.; Murnen, H.K.; Zuckermann, R.N.; Segalman, R.A. Control of Crystallization and Melting Behavior in Sequence Specific Polypeptoids. *Macromolecules* **2010**, *43*, 5627–5636.
30. Aoi, K.; Nakamura, R.; Okada, M. Polypeptide-synthetic polymer hybrids, 2. Miscibility of poly(vinyl alcohol) with polysarcosine. *Macromol. Chem. Phys.* **2000**, *201*, 1059–1066.
31. Rettler, E.F.J.; Kranenburg, J.M.; Lamberton-Thijs, H.M.L.; Hoogenboom, R.; Schubert, U.S. Thermal, Mechanical, and Surface Properties of Poly(2-N-alkyl-2-oxazoline)s. *Macromol. Chem. Phys.* **2010**, *211*, 2443–2448.
32. Fox, T.G.; Flory, P.J. The glass temperature and related properties of polystyrene. Influence of molecular weight. *J. Polym. Sci.* **1954**, *14*, 315–319.
33. Claudio, P.; Létoffe, J.M.; Camberlain, Y.; Pascault, J.P. Glass transition of polystyrene *versus* molecular weight. *Polym. Bull.* **1983**, *9*, 208–215.
34. Überreiter, K.; Kanig, G. Self-plasticization of polymers. *J. Colloid Sci.* **1952**, *7*, 569–583.
35. Lee, C.U.; Smart, T.P.; Guo, L.; Epps, T.H.; Zhang, D. Synthesis and Characterization of Amphiphilic Cyclic Diblock Copolypeptoids from N-Heterocyclic Carbene-Mediated Zwitterionic Polymerization of N-Substituted N-carboxyanhydride. *Macromolecules* **2011**, *44*, 9574–9585.
36. Nam, K.T.; Shelby, S.A.; Choi, P.H.; Marciel, A.B.; Chen, R.; Tan, L.; Chu, T.K.; Mesch, R.A.; Lee, B.C.; Connolly, M.D.; Kisielowski, C.; Zuckermann, R.N. Free-floating ultrathin two-dimensional crystals from sequence-specific peptoid polymers. *Nat. Mater.* **2010**, *9*, 454–460.